MINERAL MAPPING TECHNIQUES: A CASE STUDY IN SOUTHEASTERN RAJASTHAN

Ronak Jain[1], Mrs. Richa U Sharma[2] and Dr. Anil Kumar[3]

[1, 2, 3]Indian Institute of Remote Sensing, 4- Kalidas Road, Indian Institute of Remote Sensing, ISRO, Dehradun – 248001, India,

Email: jainronak75@yahoo.in; richaupadhyay00z@gmail.com; anil@iirs.gov.in

KEYWORDS: Airborne Hyperspectral Remote Sensing, AVIRIS-NG, Minimum Noise Fraction, Spectral Angle Mapper, Mixture Tuned Matching Filtering.

ABSTRACT: High spectral resolution of hyperspectral sensors finds applications in various scientific domains like specific mineral identification and hence, capable of replacing the traditional techniques such as multispectral remote sensing and field-based approach for mineral exploration.

Airborne Hyperspectral data is used. Minimum Noise Fraction (MNF) algorithm is used for the reduction of the dimensionality of data. PPI and n-Dimensional visualization are used for the extraction of the endmembers (pure pixels). The endmembers belong to clay minerals, carbonate minerals, iron-bearing minerals and other minerals (sulphates, silicates, oxides etc.) classes. Those endmember spectra are used for the different mapping algorithms i.e. SAM, MTMF.

Different mapping algorithms illustrate the different results. SAM uses the spectral angle and MTMF maps single target with the help of matched filtering (MF) and suppresses the background while MT for detection of the erroneous positive pixels. MTMF method provides the better results than SAM. MTMF also discriminates the settlement from the mineral zones.

1. **INTRODUCTION:** Remote Sensing is a technology used for the data acquisition of the objects which are located at distance or remote regions and perform analysis for the interpretation (Sabins, 1999) of the physical attributes of the acquired data. Electromagnetic Radiation (EMR) wavelength ranges from visible to microwave region are used for the data acquisition in remote sensing (Gupta, 2003). Multispectral remote sensing imagery pixels are having discrete spectral bands (Ting & Fei, 2012), so it is not much helpful for detection of the minerals of same classes (Pippi, 1989). Hyperspectral Remote sensing is much helpful for the detection and mapping of different minerals of same classes (Swayze et al., 1992). It provides spatial as well as spectral contiguous bands of the earth surface for mineral mapping (Goetz et al., 1985). Spectral bands of a pixel give the precise and accurate information about the objects. High spatial resolution (2-20 m) and high spectral resolution (5 -10 m) data are provided by the airborne sensors (Kruse, 2002; Kruse, Boardman, & Huntington, 2003).

2. RESEARCH DATASET AND AREA:

2.1 Dataset Used:

2.1.1 Airborne Visible/Infrared Imaging Spectrometer Next Generation (AVIRIS-NG): AVIRIS-NG instrument has been developed by Jet Propulsion Laboratory (JPL) of NASA. This is ground based as well as the airborne instrument. It has been developed to provide continued access to high signal-to-noise ratio (Dennison et al., 2013; Hamlin et al., 2011).

AVIRIS-NG measures reflected electromagnetic energy of the wavelength range from 380 nm to 2510 nm (Hamlin et al., 2011) with a narrow bandwidth of 5 nm for spectral sampling. It is across track (whisk broom) imaging spectrometer. Spatial resolution is of 8.1 m and having 425 bands for a better approach.

2.1.2 ASD FieldSpac4 Spectroradiometer: The ASD FieldSpac4 Spectroradiometer covers the range of wavelength 350 nm to 2500 nm and having three different spectral resolution sensors 3 nm (350-1000 nm), 10 nm (1000-1800 nm), and 10 nm (1800-2500 nm).

2.2 Research Area:

2.2.1 Location: The study area located near to Jahazpur city of Bhilwara district in Rajasthan, India. The study area extends from latitude 25º26'34.80" to 25º30'7.20" in the North and longitude 75º10'22.80" to 75º14'16.80" in the East of the south-eastern part of Jahazpur city. The study area is shown in Figure 1.

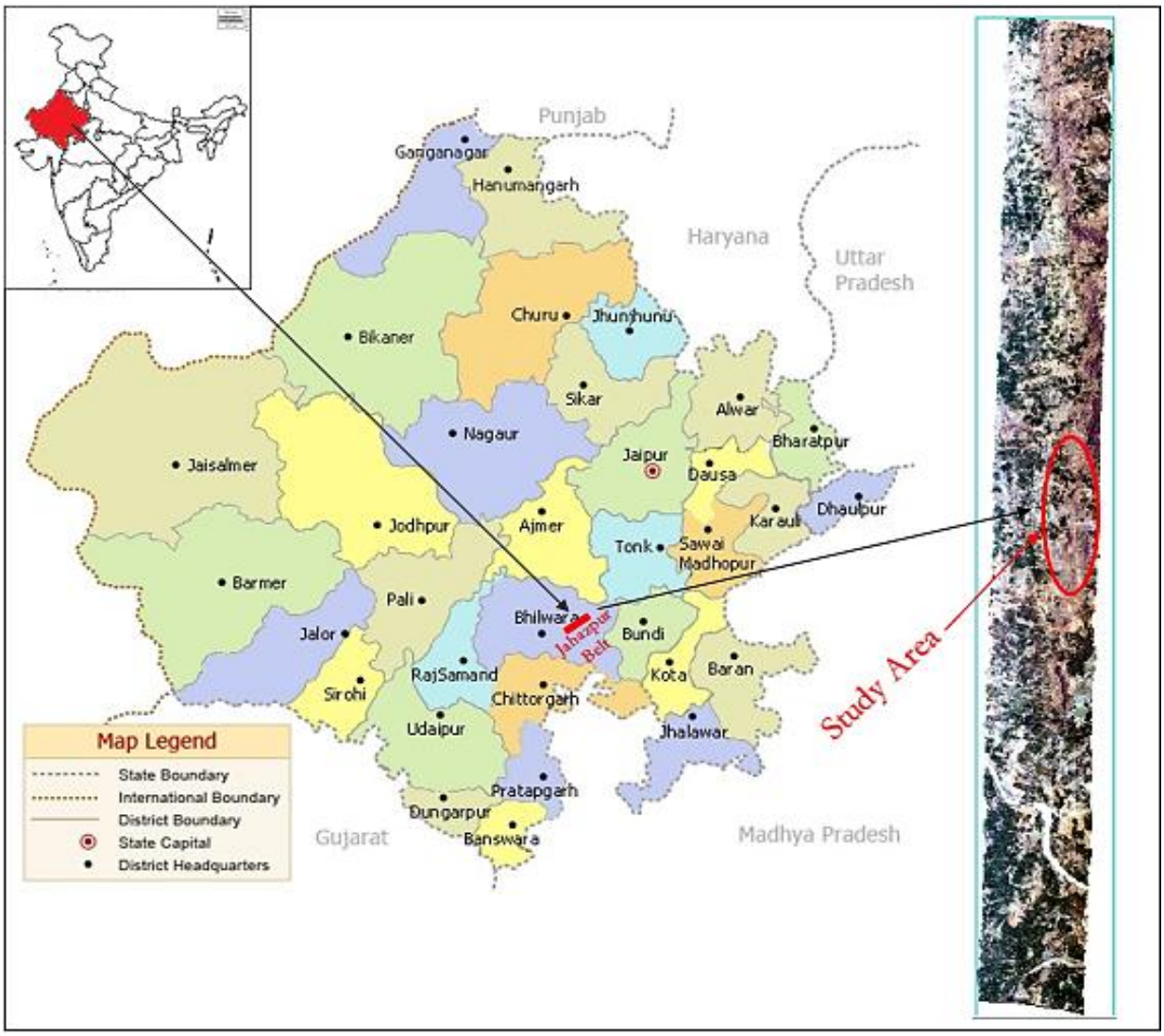

Figure 1: Study Area (Jahazpur)

2.2.2 Regional Geology: The Precambrian geology of Rajasthan is earlier studied by Coulson, (1933), Gupta, (1934), Gupta & Mukherjee, (1938), Heron, (1936), and Heron, (1953), it helped to create a basic framework. Heron, (1953) had a most significant contribution for the erection of basic framework of Precambrian geology. The antiquity in the basement rocks was first recognized by Heron, (1953).

Bhilwara Supergroup is the oldest geological record in Rajasthan region. It contained the rocks in the south-central part of Rajasthan. The geologist Gupta et al., (1981) had considered the Sandmata Complex, Mangalwar Complex, and Hindoli Group and their sub-divisions, as a part of basement region so they considered that groups into Bhilwara Supergroup. The trend of the BSG rocks is NNE-SSW. The geological map is digitized by using the District Resources Map of Bhilwara (GSI, 1998). The digitized geological map of the study area is illustrated in Figure 2.

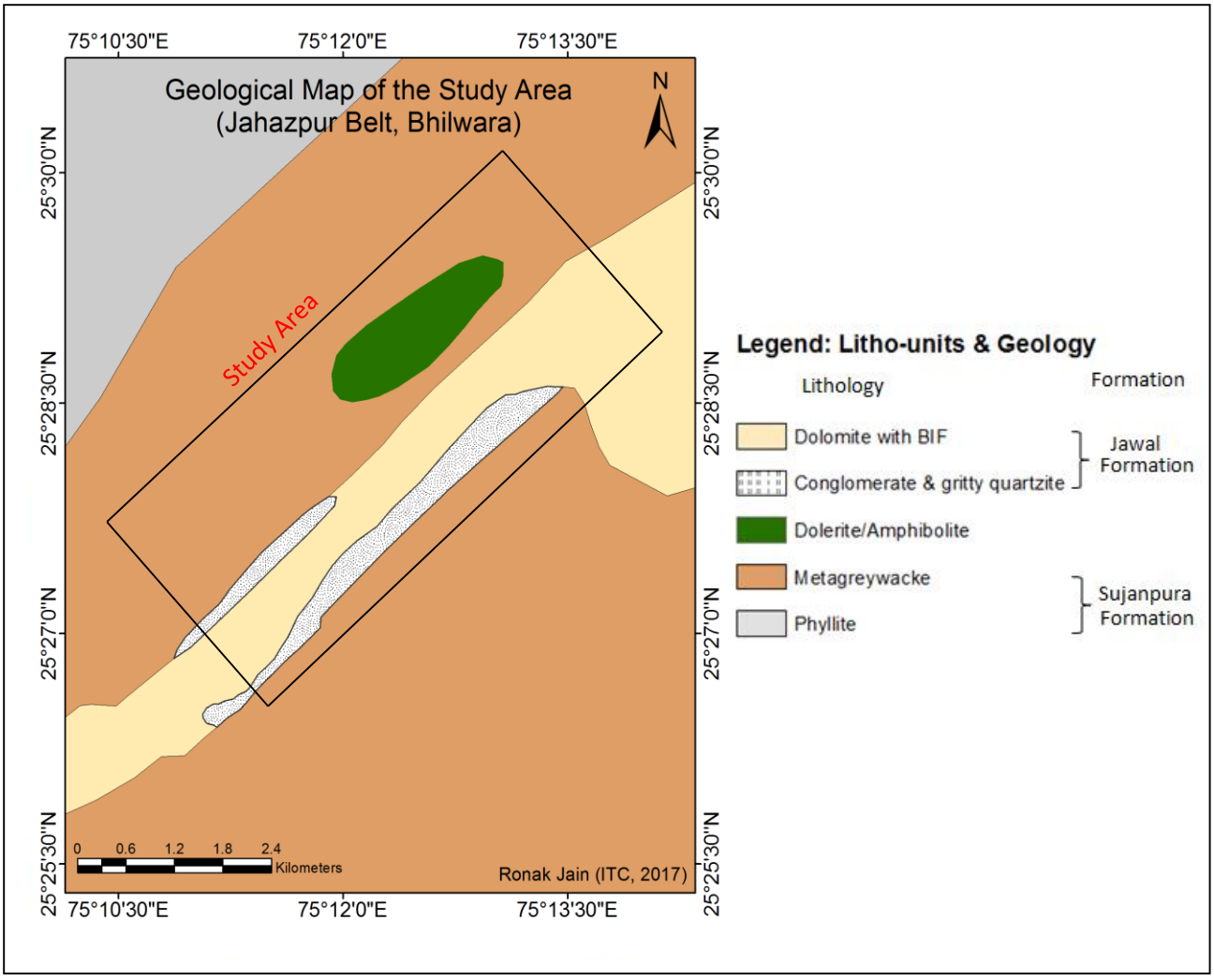

Figure 2: Digitized Geological Map of the Area

Stratigraphy: The stratigraphic sequence of the Bhilwara Supergroup is given by Gupta et al., (1997). The stratigraphy of the study area of BSG is described in Table 1:

a. Hindoli Group: The Hindoli Group located around 20 Km north-west of Bundi. It comprises of greenschist (low-grade) sequences. The Hindoli belt has trended in the southern part is NNW-SSE while in the northern part it got changed to ENE-WSW. Change of the trend in the northern region is confined within two Ductile Shear Zones (DSZ), running sub-parallel to the Hindoli's regional axial trend.

The major lithologies of this group are metavolcanics along with slate, shale, phyllite, dolomite, quartzite, mica schist and limestone. Lithofacies are also recorded in the Hindoli Group (Shrivastava, 2011).

Table 1: Stratigraphy of the Study Area. Source: (GSI, 2004)

Age	Supergroup	Group	Formation	Lithology
Lower Proterozoic	Bhilwara Supergroup	Jahazpur Group	Ummedpura Formation	Carbonaceous/purple phyllite Orthoquartzite Dolomite Grey phyllite (tuff) & dolomite with BIF Conglomerate/gritty quartzite
			Jawal Formation	Dolomite with BIF Conglomerate & gritty quartzite
Archean		Hindoli Group	Sujanpura Formation	Metagreywacke Phyllite ± garnet

b. Jahazpur Group: Lithoassemblages (coarse clastics, carbonates, pelite and iron formation) of the Jahazpur Group is unconformably overlies the rocks of the Hindoli Group. The trend of the Jahazpur Group rocks is NNE-SSW. Rocks of Jahazpur Group is in the form of two linear belts. Each of the belts is having a length of around 70 Km and width is 3 Km at the widest region. The turbidite-volcanic sequence is associated with the Hindoli Group in the eastern belt while the western belt unconformably overlies the rocks of Hindoli Group and it is extended from Jawal (SW) to Dhanola (NE).

BIF, carbonaceous phyllite, dolomitic marble, breccia, chert, arkose mica schist, orthoquartzite, gritty quartzite and polymictic conglomerate are the major litho-assemblages of the Jahazpur Group.

3. **METHODOLOGY:** The AVIRIS-NG consist of the 425 contiguous bands in which spectral data along with the noise is present so **Data Preprocessing** is required for the noise management. Along with the noise management, water absorption bands are also removed. **Minimum Noise Fraction (MNF)** is done for the reduction of the dimensionality of the data because hyperspectral data consist of the greater amount of the spectral information but the volume of data is very huge. Green et al., (1988) developed the MNF transform for ordering components in the form of image qualities. They had chosen a new component to adequately increase (maximize) the SNR and images are arranged with the increasing quality/decreasing noise. It is a modified form of Principal Component Analysis (PCA). MNF transformation divided the data space into two subspaces: (a) components having large eigenvalues (signal subspace) and (b) components having eigenvalues approximately one and noise is dominated (noise subspace). Boardman, Kruse, & Green, (1995) proposed the algorithm of **Pixel Purity Index (PPI)**. It is widely used for the extraction of endmembers from hyperspectral imagery. To find the spectrally pure (unique) pixels from the dataset, PPI algorithm plays an important role. **n-Dimensional (n-D) visualizer** is an interactive procedure for the extraction of the pure pixels (endmembers)

spectra from the spectral mixing space (Boardman & Kruse, 2011). According to Boardman, (1993), points to be considered as spectra in the n-dimensional scatterplot, n represents the number of bands. Count of the spectrally pure endmembers and their spectral signatures are estimated on the basis of the points distribution in n-dimensional space (Boardman, 1993; Boardman & Kruse, 2011; Boardman et al., 1995). The **Spectral Angle Mapper (SAM)** was developed to compute the similarities of spectrum between the unknown material reflectance spectra with reference material reflectance spectra. SAM works on an assumption that every pixel of an image belongs to a particular ground cover class and uniquely fall under that category (Addamani & Venkat, 2014). SAM computes the angle between the test (pixel/unknown) spectra and reference spectra (as shown in Figure 3) by assuming them as vectors in the space of n-D, it expressed in the following equation 1:

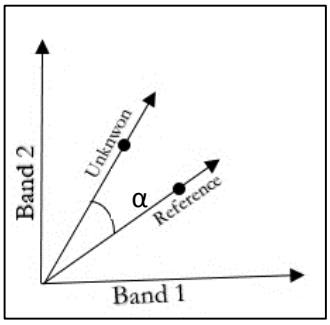

Figure 3: Spectral Angle Mapper (SAM)

$$\propto = \cos^{-1}\left(\frac{\sum_{i=1}^{n} t_i\, r_i}{\sqrt{\sum_{i=1}^{n} t_i^2}\sqrt{\sum_{i=1}^{n} r_i^2}}\right) \qquad (1)$$

Where:
α = spectral angle,
n = number of bands,
t = unknown (test) spectrum,
r = reference spectrum

Boardman, (1998) had developed the **Mixture Tuned Matched Filtering (MTMF)** technique. MTMF is a sub-pixel (partial) based algorithm. It is a combination of the Linear Spectral Mixing (LSM) model and the Matched Filtering (MF) model.

The MTMF algorithm mainly consists of the three steps (Goodarzi Mehr et al., 2013):

a. Apparent reflection data to get an MNF transformation (Green et al., 1988).
b. For the estimation of the abundance, MF is done.
c. MT for identification of the erroneous positive pixels (Boardman, 1998).

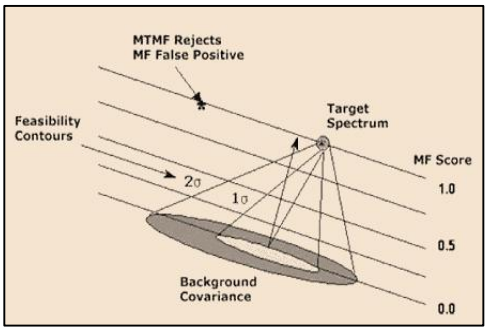

Figure 4: Working of MTMF. Source: (Boardman & Kruse, 2011)

The capability of the MF technique is to map single target (known) and to avoid the other endmembers which are in the background (as shown in Figure 4). MT is the unique and most powerful aspect of the MTMF method. MT allows the detection and rejection of the erroneous positives that are similar in the MF outcomes (Boardman, 1998).

4. RESULTS & DISCUSSION: The Spectral Angle Mapper and Mixture Tuned Matched Filtering algorithm are applied to the imagery. Both the algorithms are giving a different kind of result. SAM works on the matching of the spectral angle between unknown material and reference material while MTMF works with MF

for mapping of target and MT used for the rejection of the erroneous positives. In these study total, 13 different kinds of minerals are identified and mapped on the basis of above-mentioned algorithms.

a. Comparison of Classified Maps on the basis of Minerals:

These maps are compared on the basis of the presence and absence of different kind of minerals. Total 13 minerals are mapped by both the algorithm but their presence and absence are slightly different in the maps. SAM algorithm less classify the iron minerals (pyrrhotite and limonite) as compared to the MTMF. Area of the iron ore belt is mostly covered by the clay minerals in SAM (Figure 5A) while MTMF classified map shows a better representation of the iron ore (Figure 5B). In MTMF mixture of iron ore with the clay minerals are very less.

Clay minerals (Kaolinite and Smectite) are abundant in the study area. SAM algorithm has mapped majority of the area with clay minerals (Figure 5A). Many minerals of other classes get considered in the clay mineral class. MTMF algorithm is very helpful to distinguish the clay minerals from the minerals (Figure 5B). It mapped the clay minerals with greater accuracy than the SAM algorithm.

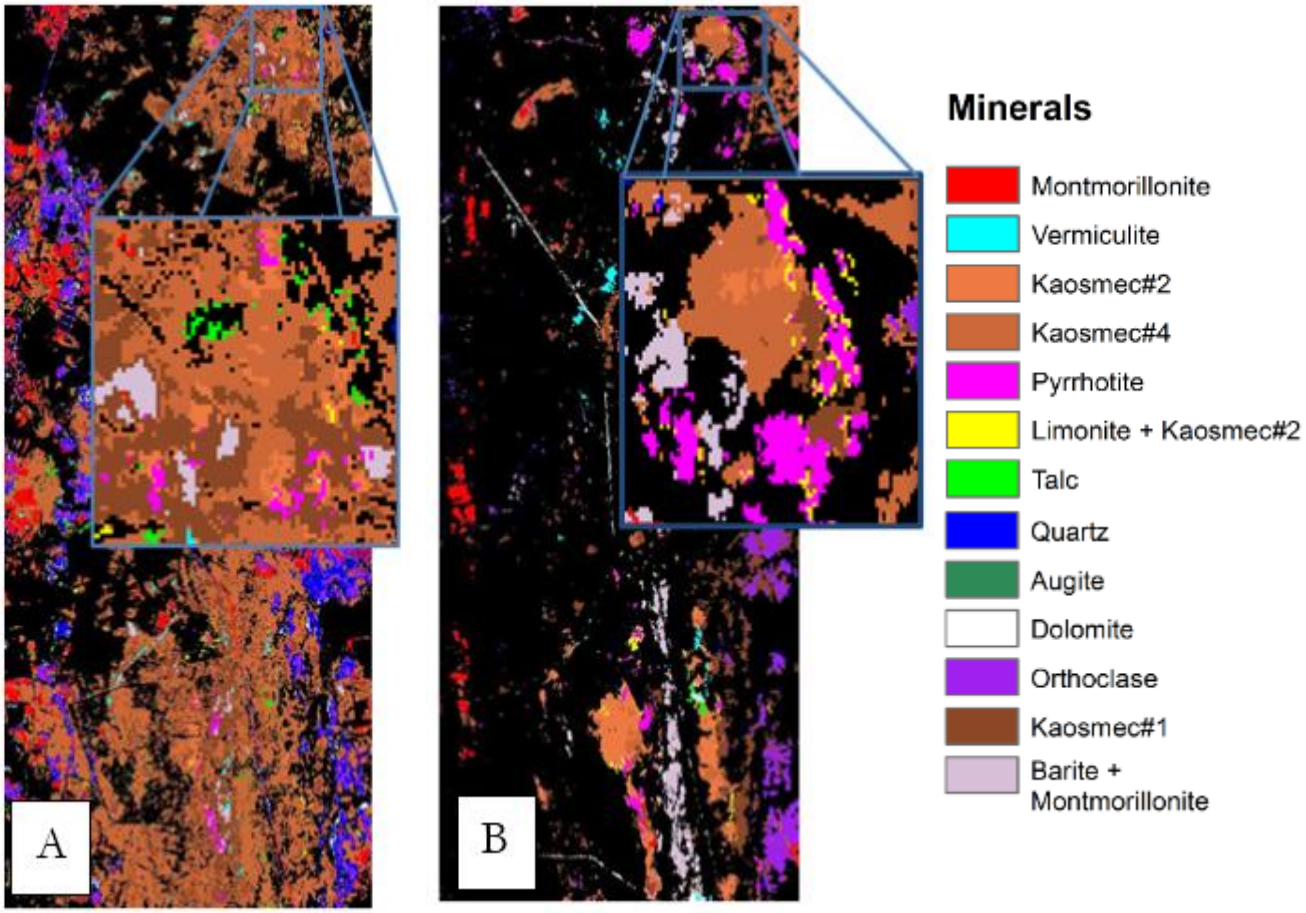

Figure 5:Comparison of minerals. A. SAM Classified Map. B. MTMF Classified Map

b. Discrimination of Settlement from the mineral zone:

Settlement zones are made of the rocks found nearby to the region. SAM classified map is not being able to discriminate the settlement to the mineral bodies (Figure 6A). Settlement zones are classified as a mineral body. Most of the settlement regions are fall under the clay mineral class. While MTMF classified map is not like the SAM classified map. Settlements are separate from the mineral bodies but 100% separation is also not possible from the MTMF (Figure 6B). MTMF classified map is much better than the SAM classified map.

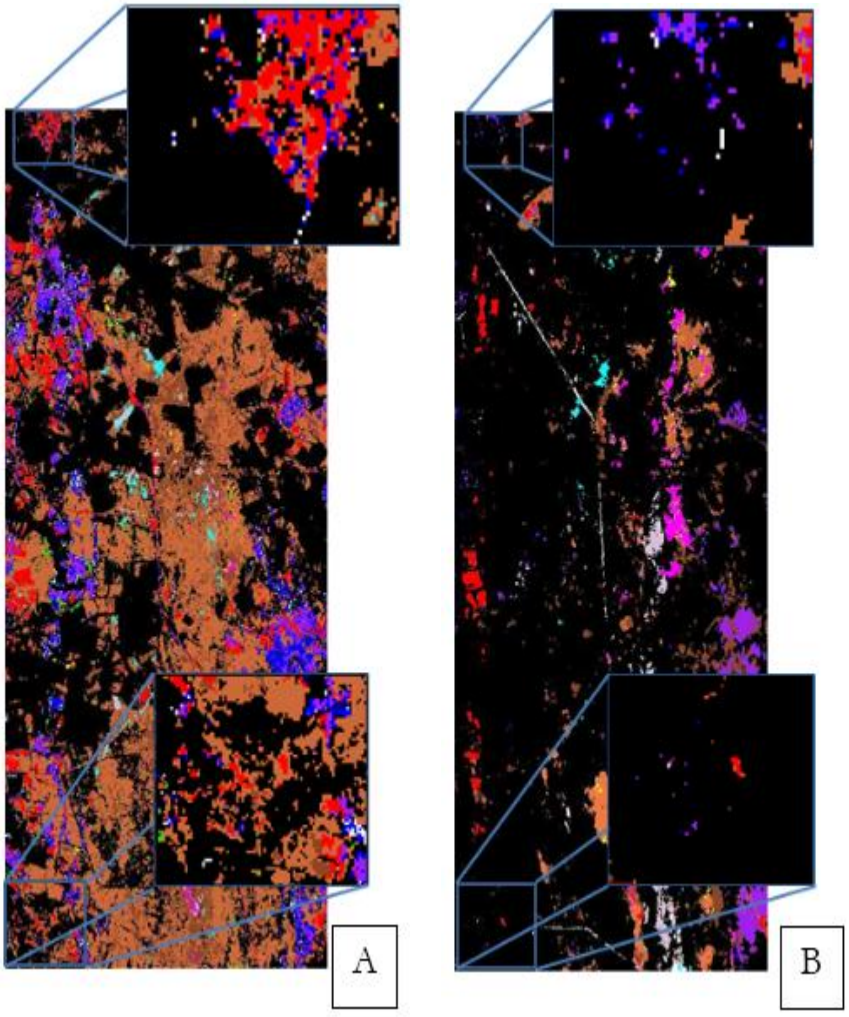

Figure 6: Discrimination of the settlements from mineral body. A. SAM Classified Map. B. MTMF Classified Map

5. CONCLUSION: Minerals are identified from the imagery are clay minerals, iron ore minerals and few other minerals. Minerals are mapped using the Spectral Angle Mapper and Mixture Tuned Matched Filtering algorithms. Generated mineral maps are compared to know about the suitability of algorithm for the mineral identification. MTMF algorithm mapped the minerals with higher accuracy and mixing of one mineral class to another mineral class is also not done. MTMF algorithm gives good results as compared to SAM algorithm. It maps the target minerals and rejects the erroneous positive pixels.

6. REFERENCES:

Boardman, J. W. (1993). Automating spectral unmixing of AVIRIS data using convex geometry concepts. In *JPL, Summaries of the 4th Annual JPL Airborne Geoscience Workshop. Volume 1: AVIRIS Workshop* (pp. 11–14). United States: JPL Publication. Retrieved from https://ntrs.nasa.gov/search.jsp?R=19950017428

Boardman, J. W. (1998). Leveraging the High Dimensionality of AVIRIS Data for improved Sub-Pixel Target Unmixing and Rejection of False Positives : Mixture Tuned Matched Filtering. In R. O. Green (Ed.), *Summaries of Seventh Annual JPL Airborne Geoscience Workshop, Volume 1: AVIRIS Workshop* (p. 55). Pasadena, California: JPL Publication.

Boardman, J. W., & Kruse, F. A. (2011). Analysis of imaging spectrometer data using N -dimensional geometry and a mixture-tuned matched filtering approach. *IEEE Transactions on Geoscience and Remote Sensing*, *49*(11), 4138–4152. https://doi.org/10.1109/TGRS.2011.2161585

Boardman, J. W., Kruse, F. A., & Green, R. O. (1995). Mapping target signatures via partial unmixing of AVIRIS data. In *Summaries of the Fifth Annual JPL Airborne Earth Science Workshop. Volume 1: AVIRIS Workshop* (pp. 23–26). United States: JPL Publication. Retrieved from https://ntrs.nasa.gov/search.jsp?R=19950027316

Coulson, A. L. (1933). The Geology of the Sirohi State, Rajputana. *Memoir of the Geological Survey of India*, *63*(1), 1–166.

Dennison, P. E., Thorpe, A. K., Pardyjak, E. R., Roberts, D. A., Qi, Y., Green, R. O., … Funk, C. C. (2013). High spatial resolution mapping of elevated atmospheric carbon dioxide using airborne imaging spectroscopy: Radiative transfer modelling and power plant plume detection. *Remote Sensing of Environment*, *139*, 116–129. https://doi.org/10.1016/j.rse.2013.08.001

Goetz, A. F. H., Vane, G., Solomon, J. E., & Rock, B. N. (1985). Imaging Spectrometry for Earth Remote Sensing. *Science*, *228*(4704), 1147–1153. https://doi.org/10.1126/science.228.4704.1147

Goodarzi Mehr, S., Ahadnejad, V., Abbaspour, R. A., & Hamzeh, M. (2013). Using the mixture-tuned matched filtering method for lithological mapping with Landsat TM5 images. *International Journal of Remote Sensing*, *34*(24), 8803–8816. https://doi.org/10.1080/01431161.2013.853144

Green, A. A., Berman, M., Switzer, P., & Craig, M. D. (1988). A Transformation for Ordering Multispectral Data in Terms of Image Quality with Implications for Noise Removal. *IEEE Transactions on Geoscience and Remote Sensing*, *26*(1), 65–74. https://doi.org/10.1109/36.3001

GSI. (1998). District Resource Map of Bhilwara. Retrieved May 19, 2017, from http://www.portal.gsi.gov.in/pls/gsipub/PKG_PTL_SEARCH_PAGES.pGetImage_PaperMap?inpRecId=1024&inpPaperMapImageId=PUB_PAPER_MAP

GSI. (2004). Kota Quadrangle. Retrieved May 19, 2017, from http://www.portal.gsi.gov.in/pls/gsihub/PKG_PTL_SEARCH_PAGES.pGetImage_PaperMap?inpRecId=1344&inPaperMapImageId=PUB_PAPER_MAP

Gupta, B. C. (1934). The Geology of the Central Mewar. *Memoir of the Geological Survey of India*, *65*, 107–125.

Gupta, B. C., & Mukherjee, P. N. (1938). Geology of Gujarat and southern Rajputana. *Rec. of the Geological Survey of India*, *73*(2), 103–208.

Gupta, R. P. (2003). Introduction. In *Remote Sensing Geology* (2nd ed., pp. 1–16). New York: Springer- Verlag Berlin Heidelberg GmbH. https://doi.org/10.1007/978-3-662-05283-9

Gupta, S. N., Arora, Y. K., Mathur, R. K., Iqballuddin, Prasad, B., Sahai, T. N., & Sharma, S. B. (1981). Lithostratigraphic map of Aravalli region, southern Rajasthan & northern Gujarat. Hyderabad: Geological Survey of India.

Gupta, S. N., Arora, Y. K., Mathur, R. K., Iqballuddin, Prasad, B., Sahai, T. N., & Sharma, S. B. (1997). The Precambrian Geology of the Aravalli region, Southern Rajasthan & North-eastern Gujarat. *Memoir of the Geological Survey of India*, *123*, 1–262.

Hamlin, L., Green, R. O., Mouroulis, P., Eastwood, M., Wilson, D., Dudik, M., & Paine, C. (2011). Imaging spectrometer science measurements for terrestrial ecology: AVIRIS and new developments. In *Aerospace Conference* (pp. 1–7). Big Sky, MT, USA: IEEE. https://doi.org/10.1109/AERO.2011.5747395

Heron, A. M. (1936). Geology of the southeastern Rajputana. *Memoir of the Geological Survey of India*, *68*(1), 1–120.

Heron, A. M. (1953). Geology of the Central Rajasthan. *Memoir of the Geological Survey of India*, *79*, 1–389.

Kruse, F. A. (2002). Mineral Mapping with AVIRIS and EO-1 Hyperion. In *Proceedings of the 11th JPL Airborne Geoscience Workshop*, JPL Publication.

Kruse, F. A., Boardman, J. W., & Huntington, J. F. (2003). Comparison of Airborne Hyperspectral Data and EO-1 Hyperion for Mineral Mapping. *IEEE Transactions on Geoscience and Remote Sensing*, *41*(6), 1388–1400. https://doi.org/10.1109/TGRS.2003.812908

Pippi, I. (1989). Mineral identification by the AVIRIS data. In *Geoscience and Remote Sensing Symposium, 1989. IGARSS'89. 12th Canadian Symposium on Remote Sensing., 1989 International* (pp. 944–947). Vancouver, Canada, Canada: IEEE. https://doi.org/10.1109/IGARSS.1989.579045

S, R., Addamani, S., Venkat, & S, R. (2014). Spectral Angle Mapper Algorithm for Remote Sensing Image Classification. *International Journal of Innovative Science, Engineering & Technology*, *1*(4), 201–205. Retrieved from www.ijiset.com

Sabins, F. F. (1999). Remote sensing for mineral exploration. *Ore Geology Reviews*, *14*(3–4), 157–183. https://doi.org/10.1016/S0169-1368(99)00007-4

Shrivastava, P. (2011). *Geology and Mineral Resources of Rajasthan*. (P. Gupta & G. Malhotra, Eds.) (3rd Revised, Vol. 30). Jaipur: Director General, Geological Survey of India, Kolkata.

Swayze, G., Clark, R. N., Kruse, F., Sutley, S., & Gallagher, A. (1992). Ground- truthing AVIRIS mineral mapping at Cuprite, Nevada. In *JPL, Summaries of the Third Annual JPL Airborne Geoscience Workshop. Volume 1: AVIRIS Workshop* (pp. 47–49). United States: JPL Publication.

Ting-ting, Z., & Fei, L. (2012). Application of Hyperspectral Remote Sensing in Mineral Identification and Mapping. In *2nd International Conference on Computer Science and Network Technology* (pp. 103–106). Changchun, China.